

## **Effect of biofilm on fluorescence measurements derived from fast repetition rate fluorometers (FRRF)**

**Jagdish S. Patil<sup>1,2,3</sup> and Toshiro Saino<sup>2,4</sup>**

<sup>1</sup>Biofouling&Bioinvasion Division, CSIR- National Institute of Oceanography, Dona Paula, Goa 403 004, India

<sup>2</sup>Hydrospheric Atmospheric Research Center, Nagoya University, Furo-cho, Chikusa-ku, Nagoya 464-8601, Japan

<sup>3</sup>Graduate School of Environmental Studies, Nagoya University, Furo-cho, Chikusa-ku, Nagoya 464-8601, Japan

<sup>4</sup>Japan Science and Technology Agency, Kawaguchi, Japan

Corresponding author

Email : [patilj@nio.org](mailto:patilj@nio.org)

Abstract: This study evaluates for the first-time, the influence of biofilms on single and double optical windows (SOW and DOW, respectively) fast-repetition-rate-fluorometer (FRRF) measurements of microalgal photosystem-II initial-fluorescence ( $F_0$ ), maximum-fluorescence ( $F_m$ ), variable-fluorescence ( $F_v = F_m - F_0$ ), quantum-yield ( $F_v/F_m$ ) and functional-absorption-cross-section ( $\sigma_{PSII}$ ). Biofilms with chlorophyll  $>0.1\mu\text{gcm}^{-2}$  and  $>0.3\mu\text{gcm}^{-2}$  on SOW and DOW, respectively, produced substantial increase in fluorescence. However, relative magnitude of biofouling effects depended on sample chlorophyll concentrations, being more critical at concentrations  $<1\text{mgm}^{-3}$ . In DOW-FRRF, biofilms affected  $F_0$  (increased) and  $F_v/F_m$  (decreased) but not  $F_v$  and  $\sigma_{PSII}$  whereas in SOW-FRRF, biofilms increased fluorescence and showed variable effect on  $F_v/F_m$  and  $\sigma_{PSII}$  because biofilms only on SOW attained real  $F_m$ . As a result, biofilm effect was substantial on SOW-FRRF measurements. On the other hand, the neutral-density-filters (representing non-chlorophyll containing biofilms) with different transmission levels reduced the fluorescence signal. The corrections procedure for the above photosystem-II parameters are also proposed here.

## Introduction

Biofouling of artificial structures is a serious problem in the marine environment resulting in vast economic losses. The term ‘biofouling’ refers to the undesired accumulation of micro- and macro-organisms on any artificial structure (Cooksey & Cooksey 1995). In recent years, as a part of continuous ocean monitoring programs, several optical marine instruments such as spectrophotometers, fluorometers, underwater cameras etc., are deployed on a long-term basis for obtaining nearly continuous observations. Regardless of such technological advances, biofouling of an optical window (OW) is one of the most serious problems hindering their long-term operations, especially in the coastal environments. Algal biofouling on the OW of optical back scatterance sensors in Tampa Bay, Florida, limited the instrument deployment period to less than a week (Schoellhamer 1993). Miller et al. (1996) described an *in situ* benthic temperature, light and horizontal water speed recorder designed for deployment periods of up to 3 months. However in tests, measurements from the light sensor after a period of 12 days were no longer accurate due to biofilm formation on the sensor surface (Miller et al. 1996). Similarly, Kerr et al. (1998) demonstrated that the early stages of biofouling, mostly by algae, can affect the performance of the optical sensors such as chlorophyll fluorometer and transmissometer. Until recently, the biofouling effect on the optical instrument data has in most cases not been tested or quantified. So in this study, the effect of natural biofilms on the performance of optical instruments is addressed, using fast repetition rate (FRR) fluorometry (Falkowski & Kolber 1995) as a representative instrument.

Over the last decade, the growing use of FRR fluorometer (FRRF) has provided insights into the factors controlling the variability in phytoplankton photosynthetic parameters and gross primary production *per se*. FRRF offers rapid, real time and *in situ* measurements of photosynthetic characteristics of natural assemblages of marine and freshwater phytoplankton populations (eg Moore et al. 2003 & 2005, Kaiblinger & Dokulil 2006, Mino et al. 2013) as well as on the reef building corals (Lesser & Gorbunov 2001). The basis of FRRF technique is to measure fluorescence transients induced by a rapid train of sub-saturating excitation flashlets, where the intensity, duration, and time delay between them can be individually controlled (Kolber et al. 1998). Interpretation of fluorescence transients (Figure 1a) induced by FRR excitation protocols allow calculation of a range of photosynthetic parameters such as; initial ( $F_0$ ), maximum ( $F_m$ ) and variable ( $F_v = F_m - F_0$ ) components of photosystem II (PSII) fluorescence, quantum yield ( $F_v/F_m$ ), functional absorption cross-section ( $\sigma_{PSII}$ ) and the kinetics of electron transfer

on the acceptor side of PSII. *In situ*, FRRF measures the above photosynthetic parameters in both light and dark-adapted states. Incorporating the measured photosynthetic parameters in appropriate models relating fluorescence and photosynthesis allows calculation of photochemical/non-photochemical quenching, photochemical conversion efficiency and gross oxygen production (Kolber & Falkowski 1993). At present, FRRF with single and double OW are used *in situ* for studying spatial and temporal variability in phytoplankton photosynthetic parameters and primary productivity (Figure 1). FAST<sup>tracka</sup> (Chelsea Technologies Group, UK), *Diving flash* (Kimoto electric co. Ltd., Japan) and *in situ* FIRE (Satlantic LP) are FRRF with double OW (DOW-FRRF), whereas the FAST<sup>trackall</sup> and FastOcean both from Chelsea Technologies Group, UK, are FRRF with single OW (SOW-FRRF). These instruments can be successfully deployed for a wide variety of experiments on many different platforms such as moorings, profiling buoys and benthic platforms worldwide (eg. Gorbunov et al. 2001, Fujiki et al. 2008 & 2011). In a moored operation, the acquisition lifetime may be extended to the timescale of months by properly managing the instrument sleep cycles. The FRRF is powered externally either through the interface or battery pack. Because of these feasibilities, researchers are considering FRRF for long-term studies along with other sensors (eg. conductivity, temperature and depth (CTD), photosynthetically active radiation (PAR), dissolved oxygen and chlorophyll *a*).

The use of optical instruments exclusively for studying the influence of biofouling on their performance without proper antifouling measures is risky as well as expensive. During field studies, chances of the instruments optical system getting damaged are more (because of fouling or during cleaning), which becomes a costly affair to repair. Further, for such studies, it is unrealistic to use two expensive instruments for control and experimental runs. Considering the risk and cost involved in deploying or devoting an instrument for biofouling studies, a simulation of fouled OWs using natural biofilms and neutral density filters (NDF) for evaluating instrument performance is proposed. Earlier Kerr et al. (1998) studied the influence of biofouling on the optical instruments (chlorophyll fluorometer and transmissometer) performance by deploying the whole instrument. They assessed biofilm development by quantifying the biological organisms and transmission of test coupons, which were deployed with the instruments. Though biofouling extent is determined through the quantification of biological organisms, chl *a* represents a better proxy for chlorophyll fluorometers. Therefore, in this study, chl *a* concentrations and transmission levels of biofilms are considered because the former increases the fluorescence signal whereas the latter decreases the intensity of excitation light and fluorescence signals. Further, biofilm transmission measurements also takes into account the biofilm thickness and area

covered by fouling organisms or other particles, if any. Irrespective of the type of biofilms on the FRRF OW, the nature of its effect on FRRF measurements will remain same. Therefore, biofilm characterization and data reproducibility will not be an issue. However, in some cases, dominance of non-chl *a* containing organisms or particles (eg. non-pigmented bacterial biofilms) in biofilms will lead to drop in transmission levels. Earlier studies reported that natural biofilms can reduce the transmission up to 60% (Kerr et al. 1998, Patil et al. 2007, Patil & Jagadeesan 2011). In view of this, using NDF, FRRF performance was evaluated at transmission levels ranging between 10 to 80%. In this study, the methodology used to evaluate the effect of optical biofouling on FRRF performance is the first of its kind. The purpose of using the FRRF was due to the availability of two different versions having different optical designs (Figure 1).

## **Materials and methods**

All the experiments were carried out using two different versions of FRRF (FAST<sup>tracka</sup> and FastOcean) manufactured by Chelsea Technologies Group, UK. FAST<sup>tracka</sup> (first generation FRRF) is a DOW-FRRF whereas FastOcean (third generation FRRF) is a SOW-FRRF. Experiments using FAST<sup>tracka</sup> and FastOcean were conducted at Hydrospheric and Atmospheric Research Center (Nagoya University, Japan) and Biofouling and Bioinvasion Division (CSIR-National Institute of Oceanography, Goa, India), respectively.

### ***Description of FRRF optical windows (OWs)***

#### ***a. FRRF with double optical window (DOW)***

The FAST<sup>tracka</sup> optical system consists of two optical chambers, light and dark, for measuring the light and dark-adapted samples, respectively. Each chamber comprises of an excitation window (EW; 15 x 40 mm) and a detection window (DW; 10 x 15 mm), which are positioned at right angles (90<sup>0</sup>) to each other (Figure 1a). From the EW, FRRF delivers a series of saturation flashes of high intensity (20,000  $\mu\text{E m}^{-2} \text{s}^{-1}$ ) of microsecond order from a blue light emitting diode (LED) light source (Nichia; 478 nm peak emission) at a repetition rate of 200 kHz. The DW receives the fluorescence signal (at 680 nm) emitted by the phytoplankton exposed to the excitation light. Fluorescence signal is then directed by a series of prisms to a passive collimator. After collimation, the fluorescence signal is filtered through a pair of interference filters (Corion Corporation, Holliston MA, USA) and a long pass filter (Schott RG-665). Subsequently, the fluorescence signal is detected by a side-on photomultiplier tube (Hamamatsu R928). As a reference signal, a small portion of the excitation light is detected by a PIN photodiode

(Hamamatsu S1722). After digitization, the fluorescence and reference signals are transferred to a computer. The digitized reference signal and the ratio of the fluorescence to reference signal are then analyzed with the help of a custom software (FRS v1.4) provided by the instrument manufacturer.

*b. FRRF with single optical window (SOW)*

The FastOcean profiling system is comprised of ambient and dark sensors to take measurements of light and dark-adapted samples, respectively. The optical system of each sensor consists of one large circular OW from which excitation of the light as well as the detection of the fluorescence signal takes place. FRRF delivers a series of high intensity saturation flashes of microsecond order from three independently controlled LED arrays centered at 450, 530 and 624 nm, with custom filtering to minimize overlap with fluorescence detection. The same window, which is equipped with an inbuilt near infrared (NIR)-enhanced photomultiplier tube for fluorescence signal detection, receives the fluorescence signal emitted by the phytoplankton sample exposed to the excitation light.

***Variable fluorescence measurements***

FRR fluorescence transients were obtained using a single-turnover protocol that provided a flash sequence consisting of a series of 100 saturation flashlets (1.1  $\mu$ s flash duration and 2.8  $\mu$ s inter flash period) and a series of 20 relaxation flashlets (1.1  $\mu$ s flash duration and 50  $\mu$ s inter flash period). The gain was adjusted depending upon the chlorophyll *a* (chl *a*) concentration of the sample taken for measurement. Filtered seawater were used as blanks for baseline correction. The curve-fitting procedure was performed by using the software that was provided with the system.

***Development of natural biofilms***

For natural biofilm development, cover glasses (for assessing DOW-FRRF) and sterile polystyrene petri dishes (for assessing SOW-FRRF) were used considering the dimensions of the OWs. To obtain biofilms of different levels, both the surfaces were deployed in a tank containing natural water (enriched with nutrients used for preparing microalgal culturing media i.e. *f/2* media; Guillard & Ryther 1962), for different durations (up to 6-7 days). Cover glasses (25 x 60 x 0.12 mm) and polystyrene petri dishes were deployed in a tank containing natural freshwater and seawater, respectively. Fresh water was collected from fresh water pond located in Nagoya University campus whereas saltwater was collected from Dona Paula Bay located along the west coast of India. Biofilm was developed on only one side of the cover glass and inner base of the polystyrene surfaces. Both these surfaces with different aged

biofilms (here after referred as natural biofilms) were retrieved for the FRRF measurements of microalgal cultures and filtered seawater in bench top mode and natural water in *in situ* mode. The details of FRRF measurements and the placing of natural biofilms on OWs are provided in the section ‘Mode of FRRF operations’.

### ***Assessment of natural biofilms***

Prior to FRRF measurements, the transmission spectra (400-750 nm) of the fouled surfaces were measured by using UV-visible spectrophotometer as described by Kerr et al. (1998). Shimadzu MPS 2000 and Shimadzu UV-2550 fitted with an integrated sphere were used for cover glasses and polystyrene surfaces, respectively. Fouled surfaces were air-dried before transmission measurements so that the results could be averaged for the surface area. Air drying of the biofilms did not affect the chl *a* concentrations as evident from the linear relationship between measured chl *a* and the biofilm transmission at 680 nm (a wavelength for chl absorption). The results are an average of 3 to 5 spectral scans for which the clean (new) surfaces served as the reference. In this study, transmission levels at 478 and 680 nm were considered because the FRRF excites blue light at 478 nm to saturate phytoplankton PSII and the detector receives fluorescence signals at 680 nm.

For biofilm chl *a* measurements, fouled surfaces were scraped with a soft brush in a known volume (35 ml) of filtered (0.22 µm Millipore) seawater. The scraped material was filtered onto 25 mm GF/F filter paper, which was then subjected to N, N-dimethylformamide (for cover glass samples) and 90% acetone (for polystyrene samples) for pigment extraction overnight (Suzuki & Ishimaru 1990). The chl *a* concentrations were measured by using Turner designs fluorometers (models: AU-10 and Trilogy) and the values are expressed as µg cm<sup>-2</sup>. AU-10 and Trilogy were used for the samples obtained from the cover glasses and polystyrene surfaces, respectively.

### ***Mode of FRRF operations***

A flow-chart describing in detail the mode of (a) DOW-FRRF and (b) SOW-FRRF using natural biofilms containing the chlorophyll is illustrated in the figure 2.

#### ***a. Mode of operations in DOW-FRRF***

In DOW-FRRF, operations using light chamber were made in the bench-top as well as *in situ* mode to confirm that the biofilm effects are similar in both the modes. In bench-top mode, biofilm effect on the FRRF measurements of laboratory grown cultures of a microalga (Prymnesiophyceae - *Isochrysis*

*galbana*) and 0.22  $\mu\text{m}$  filtered seawater (as blank) was evaluated using a cuvette. In the *in situ* mode, measurements were taken with and without biofilms on OWs by deploying DOW-FRRF in a tank containing natural fresh water (data not shown). In both the modes, measurements of samples (filtered seawater, microalgal culture and natural water) were taken by placing different levels of natural biofilms on the OWs. Similarly, measurements of the microalgal cultures and filtered seawater were also made using NDF of different transmission levels (80, 60, 50, 40 and 10%) instead of natural biofilms. In DOW-FRRF, the natural biofilms (air dried) and NDF were placed on the OWs with the help of water proof adhesive tape. While placing the fouled cover glass, extreme care was taken to ensure that the biofilm layer was facing outside and the opposite side towards OW. The readings obtained using clean cover glasses were considered as control. Additionally the effect of presence of biofilms and NDF on either EW or DW was also evaluated separately in the bench top mode. The effect of presence of biofilms or NDF on FRRF OWs (both windows and either on EW or DW in DOW-FRRF) were conducted separately in triplicates. Further, the FRRF measurements of seawater made in the presence and absence of biofilms of known chl *a* concentrations were used to determine biofilm thresholds. The measurements made in the absence of biofilms were considered as control.

*b. Mode of operations in SOW-FRRF*

In SOW-FRRF, the instrument was fixed in the vertical position to a profiling frame and the measurements were made by keeping the polystyrene petri dishes (with and without live biofilms) containing sample and NDF on the large flat OW. The readings obtained using clean polystyrene petri dishes without biofilms were considered as control. In the bench top mode, the effect of presence of biofilms and NDF on FRRF OWs were conducted separately in triplicates using cultures of *Isochrysis galbana* and filtered seawater (as blank). Filter seawater was obtained by passing natural seawater through 0.22  $\mu\text{m}$  Millipore filter paper. The FRRF measurements of filtered seawater were also made in the presence and absence of biofilms of known chl *a* concentrations to determine biofilm thresholds.

**Data analysis**

The fluorescence values ( $F_0$  and  $F_m$ ) from filtered seawater (with and without biofilms) obtained from SOW- and DOW-FRRF were then subjected to statistical test (T-test) to identify the significant differences between the control and biofilm affected data. The significantly affected fluorescence values were then matched with the corresponding biofilm chlorophyll values and the minimum fluorescence value amongst them was selected as biofilm threshold. The thresholds were determined separately for

SOW- and DOW-FRRF. The thresholds were determined only to identify the minimum chlorophyll concentration of the biofilm that significantly affected FRRF measurements.

### ***PSII parameters measured***

In this study the effect of natural biofilms and NDF on the performance of DOW and SOW FRRF was assessed through the measurements of  $F_0$ ,  $F_m$ ,  $F_v$ ,  $F_v/F_m$  and  $\sigma_{PSII}$ . The parameters of samples measured (i) without biofilms are represented by expressing “S” as a superscript (eg.  $F_0^S$ ,  $F_m^S$ ,  $F_v^S$ ,  $F_v/F_m^S$  and  $\sigma_{PSII}^S$ ) and (ii) with biofilms are represented by expressing “B+S” as a superscript (eg.  $F_0^{B+S}$ ,  $F_m^{B+S}$ ,  $F_v^{B+S}$ ,  $F_v/F_m^{B+S}$  and  $\sigma_{PSII}^{B+S}$ ). However, PSII parameters of only biofilms are represented by expressing “B” as a superscript (eg.  $F_0^B$ ,  $F_m^B$ ,  $F_v^B$ ,  $F_v/F_m^B$  and  $\sigma_{PSII}^B$ ).

## **Results**

### ***Transmission spectra and chlorophyll a concentration of biofilms***

The transmission spectra of different levels of natural biofilms developed in the laboratory are shown in the figure 3 a–b. The average transmission of the biofilms within the visible range (400 to 700 nm) varied from 99.2 to 90%. The transmission spectra indicated a distinct trough around 685 nm, which was mainly due to the absorption by chl *a*. The laboratory experimental results revealed a significant linear relationship between the biofilm chl *a* concentration and the transmission at 680 nm (Figure 3c). The chl *a* concentrations in the biofilms ranged from 0.02 to 14  $\mu\text{g cm}^{-2}$  wherein the lowest and highest concentrations were seen for the biofilms having a transmission (at 680 nm) of 99.2 and 90%, respectively (Figure 3).

### ***Influence of biofilms on FRRF OWs***

#### ***a. DOW-FRRF***

The experiments with biofilms on EW and DW revealed that the fluorescence values ( $F_0$  and  $F_m$ ) increased, variable fluorescence ( $F_v$ ) remained unchanged and the quantum yield ( $F_v/F_m$ ) decreased with the decrease in the transmission level (Figure 4). These differences were significant when the transmission of fouled coupons decreased beyond 98% (Table 1; Figure 4). The  $\sigma_{PSII}$  values showed insignificant variation with decrease in the transmission caused by natural biofilms compared to control (Figure 4). Similar results were obtained with bench top and *in situ* mode measurements.



In the bench top mode, FRRF measurements ( $F_0$ ,  $F_m$ ,  $F_v$ ,  $F_v/F_m$  and  $\sigma_{PSII}$ ) of microalga taken in the presence of biofilms only on EW showed insignificant variations compared with control i.e. without biofilms (Figure 5). The FRRF measurements ( $F_0$  and  $F_m$ ) of filtered seawater also showed insignificant variations up to the transmission levels of <98.67% (Table 1). However, when the biofilm chl *a* concentrations increased, the transmission levels decreased (up to 94.7%) and the fluorescence values ( $F_0$  and  $F_m$ ) increased significantly as compared to controls (Table 1; Figure 5). On the other hand, presence of biofilms on the DW resulted in increased  $F_0$  and  $F_m$  values with decrease in transmission and increase in biofilm chl *a* concentrations (Table 1; Figure 5). In case of cultured microalga,  $F_v$  values were similar to control whereas  $F_v/F_m$  values decreased with decrease in transmission and increase in biofilm chl *a* (Table 1; Figure 5). The  $\sigma_{PSII}$  values did not show much variation compared to control (Figure 5).

#### *b. SOW-FRRF*

Experiments conducted by placing biofilms on OW of SOW FRRF revealed contrasting results compared to DOW type FRRF. In SOW-FRRF, the fluorescence values ( $F_0$ ,  $F_m$  and  $F_v$ ) showed an increasing trend whereas  $\sigma_{PSII}$  values decreased with the decrease in transmission level and increase in the biofilm chl *a* compared to control (Figure 6a). Unlike in DOW-FRRF, the  $F_v/F_m$  did not show decreasing trend with the increase in biofilm age (Figure 6a).

#### ***Influence of neutral density filters on FRRF OWs***

The measurements of samples taken with NDF on the OW of SOW- and DOW-FRRF revealed that the values of all the parameters ( $F_0$ ,  $F_m$ ,  $F_v$ ,  $F_v/F_m$  and  $\sigma_{PSII}$ ) decreased with decrease in transmission levels (Figures 6b and 7). These findings were consistent in both, bench top and *in situ* measurements. In case of DOW-FRRF, the experiments conducted in the bench top mode by placing NDF on either EW or DW revealed that although the  $F_0$  and  $F_m$  decreased linearly with decrease in transmission, the magnitude of decrease was higher with the NDF present on the EW (Figure 8). In case of measurements made with NDF only on EW,  $F_v/F_m$  and  $\sigma_{PSII}$  decreased linearly with reduction in transmission (Figure 8). However, there was no effect on  $F_v/F_m$  and  $\sigma_{PSII}$  when the NDF was present on DW (Figure 8).

## Discussion

### Influence of biofilms and NDF on fluorescence measurements ( $F_0$ and $F_m$ )

#### *DOW-FRRF*

In DOW-FRRF,  $F_0$  and  $F_m$  values of control and with biofilms on EW were similar suggesting that the biofilm development on the EW did not influence the fluorescence measurements significantly (Figure 5). However, biofilms placed on the DW resulted in higher  $F_0$  and  $F_m$  values compared to control (Figure 5) because of chl *a* containing organisms present in natural biofilms. The distinct trough around 680 nm of the biofilm transmission spectra (wavelength for chl *a* absorption) and its linear relationship with measured chl *a* confirmed high chlorophyll in the biofilms (Figure 3c). The increase in  $F_0$  and  $F_m$  values coincided with biofilm chl *a* concentrations of  $>0.3 \mu\text{g cm}^2$  (Table 1; Figure 4) suggesting that minimum threshold will be more critical at low concentrations ( $<1 \text{ mg m}^{-3}$ ) but some effect (may not be significant) will also be observed even for samples with high chlorophyll concentrations (Table 1; Figure 4). However, for high chlorophyll samples threshold increased slightly ( $>1 \mu\text{g cm}^2$ ; Figure 4). The increase in fluorescence is because of the excitation of biofilm chl *a* on DW due to small amount of scattered LED flashlight from the blue LED light source that delivers high intensity flashes from EW to saturate phytoplankton PSII reaction center. As a result, the detector receives the signal from sample as well as biofilm algae on the DW, thus leading to overestimation of  $F_0$  and  $F_m$  values.

#### *SOW-FRRF*

SOW-FRRF also showed increase in fluorescence signals as seen in DOW-FRRF. Since the strong excitation and detection occurred from the same OW (Figure 6a) the increase in fluorescence was more pronounced than that observed in DOW-FRRF. It has been observed that the increase in  $F_0$  and  $F_m$  values coincided with biofilm chl *a* concentrations of  $>0.1 \mu\text{g cm}^2$  and  $>0.3 \mu\text{g cm}^2$  for low and high chlorophyll samples respectively (Table 1; Figure 6a). Comparison between SOW-FRRF and DOW-FRRF revealed that the biofilm chl *a* thresholds for low and high chlorophyll samples were smaller in former than latter case.

### *Influence of biofilms and NDF on variable fluorescence ( $F_v$ ) measurements*

The increase in  $F_0$  and  $F_m$  values may or may not affect  $F_v$  values [ $F_v = F_m - F_0$ ] depending on the strength of the excitation light and the status of the chl *a* in the cell. If the chl *a* is detached from the PSII reaction center (due to intensified decomposition by coexisting grazers on the biofilm or drying of the

biofilms before measurements as in present study) or not saturated by small amount of excitation light, it affects  $F_0$  and no fluorescence transient takes place. In this case, the increase in  $F_0$  and  $F_m$  values will not affect the  $F_v$  values (Figure 7) which remains same as that of control (Figure 5) and the relation will be  $F_v^{B+S} = F_v^S$ . On the other hand if the chl  $a$  is a part of PSII reaction center or saturated by strong excitation light, it affects  $F_0$  as well as  $F_m$  (when used with natural biofilms without drying). In this case,  $F_v$  of the fouling algae may be different from the sample algae and the relation is  $F_v^{B+S} > F_v^S$ .

#### *DOW-FRRF*

In DOW-FRRF, small amount of excitation light excites but did not saturate the biofilm chlorophyll on the DW. In this study though air drying of biofilms might affect the fluorescence properties, it still did not affect the results. Therefore the signal obtained will not show any  $F_v$  even if biofilm chlorophyll is photosynthetically active (i.e.  $F_0 = F_m$ ) because the biofilms on OW will not attain real  $F_m$  i.e.  $F_v$  values are same as that of control (Figure 4) and the relation is  $F_v^{B+S} = F_v^S$ . However, in the presence of NDF, the  $F_0$  and  $F_m$  values decreased linearly with decrease in transmission levels (Figure 8). This suggests the effect of non-chlorophyll containing biofilms on FRRF performance because of decrease in optical transmission.

#### *SOW-FRRF*

Considering the optical design, the relation in SOW-FRRF will be  $F_v^{B+S} > F_v^S$  and this is because the LED excitation light hitting the biofilm was strong (because excitation and fluorescence detection occurred from the same window) to take the fluorescence transient similar to the algae. These observations confirm that the biofilms in SOW-FRRF attain real  $F_m$  but not in DOW-FRRF as a result  $F_v$  values were higher compared to sample (Figure 6a). Further in the presence of NDF, the fluorescence values decreased linearly with decrease in transmission levels as observed in DOW-FRRF (Figure 6b)

#### ***Influence of biofilms and NDF on quantum efficiency ( $F_v/F_m$ )***

$F_v/F_m$  is a measure of photosynthetic quantum efficiency (Kolber et al. 1988, Kolber et al. 1990) and ranges from 0.2 to 0.65. Low  $F_v/F_m$  relates to the fraction of PSII reaction centers that are functionally damaged (Greene et al. 1992) or photoinhibited (Kraus & Weis 1991). However,  $F_v/F_m$  from fouled FRRF OWs cannot be linked to phytoplankton physiology as the physiological status of biofilm chl  $a$  (as explained above) will interfere with the measurements.  $F_v/F_m$  will be low when biofilm chl  $a$  is

detached from the PSII reaction center (affects only  $F_0$  i.e.  $F_0^{B+S} > F_0^S$ ) or variable if attached to the PSII reaction center (affects  $F_0$ ,  $F_m$  and  $F_v$  i.e.  $[F_0^{B+S}, F_m^{B+S}, F_v^{B+S}] > [F_0^S, F_m^S, F_v^S]$ ).

#### *DOW-FRRF*

In DOW-FRRF,  $F_v/F_m$  was not affected by the presence of biofilms on EW. This suggests that the reduction in light transmittance by biofilms on EW was not great enough to reduce the LED flash intensity to a level not sufficient to cause single turnover measurements (Figure 5). However, the low  $F_v/F_m$  observed in the presence of biofilms on the DW cannot be attributed to phytoplankton physiology (Figure 5). The increase in the  $F_0$  value due to the presence of biofilm algae on the DW was most likely responsible for the low  $F_v/F_m$ .  $F_v/F_m$  also remained unchanged in the presence of NDF on DW (Figure 8).

#### *SOW-FRRF*

Unlike in DOW-FRRF,  $F_v/F_m$  did not decrease in SOW-FRRF (Figure 6a) because the signal from the biofilm showed  $F_v$  component similar to the phytoplankton sample. However, when the fluorescence signal from the biofilm was several times higher than the signal from the sample, the recorded  $F_v/F_m$  reflected the photosynthetic status of biofilm rather than the sample.

#### ***Influence of biofilms and NDF on functional absorption cross-section ( $\sigma_{PSII}$ )***

The  $\sigma_{PSII}$  describes the efficiency of light utilization for photochemistry in PSII. It is the product of the light-harvesting capability of the light-harvesting pigments and the efficiency of excitation transfer to the reaction center (Ley & Mauzerall 1982, Mauzerall & Green-Baum 1989, Dubinsky 1992). The  $\sigma_{PSII}$  is derived from the rate of increase between  $F_0$  and  $F_m$  fluorescence (Figure 7) and any variations in this rate will affect  $\sigma_{PSII}$  values. *In situ*  $\sigma_{PSII}$  is largely determined by the fluorescence yield contributed by the dominant species within a mixed species assemblage (Suggett et al. 2004). Hence, biofilm chl *a* may or may not interfere with  $\sigma_{PSII}$  measurements depending on the presence of organisms (taxa and physiological status) and type of FRRF used. If biofilm chl *a* is dead or detached from the PSII reaction center (i.e. when  $F_v^{B+S} = F_v^S$ ), then  $\sigma_{PSII}$  is unaffected and less susceptible to fouling.  $\sigma_{PSII}$  will be variable if biofilm chl *a* is live or remains attached to PSII reaction center (i.e. when  $F_v^{B+S} > F_v^S$ ) and will also depend on the physiological status and nature of organisms present in the biofilm and the water sample. Laboratory studies indicated that  $\sigma_{PSII}$  was more variable between taxa and hence the mixing of population will be a crucial determinant *in situ* (Suggett et al. 2004). Based on the mixing experiments

conducted by Suggett et al. (2004), it is presumed that the  $\sigma_{\text{PSII}}$  will either change proportionally (if  $F_m^B = F_m^S$  or  $F_m^{B+S} = 2 * F_m^S$ ) or disproportionately (if  $F_m^B \neq F_m^S$ ) depending on the  $F_m$  values of the populations present in the biofilm ( $F_m^B$ ) and water samples ( $F_m^S$ ). However,  $\sigma_{\text{PSII}}$  will change little from the value exhibited by the population with the  $F_m$ , until the mixing ratio approaches an approximately equivalent fluorescence yield for biofilms and water samples.

#### *DOW-FRRF*

In DOW-FRRF, biofilms on EW caused minimum variations in the  $\sigma_{\text{PSII}}$  when compared to control (Figure 5). However, in the presence of NDF on the EW of DOW-FRRF, the  $\sigma_{\text{PSII}}$  values decreased linearly with decrease in transmission compared to control (Figure 8). This is because the NDF on EW decreases the intensity of LED excitation light. The decrease in flash intensity not only decreased the fluorescence signals ( $F_0$  and  $F_m$ ; Figure 8) but also delayed PSII saturation of the sample algae. Although during this study, transmission reduction caused by the biofilms at EW was not sufficient to affect  $\sigma_{\text{PSII}}$  but significant decrease in transmission due to increased biofouling can affect  $\sigma_{\text{PSII}}$ . The presence of biofilm or NDF on the DW of DOW-FRRF did not influence the  $\sigma_{\text{PSII}}$  values when compared to control (Figure 8). This is because the DW receives a lowered fluorescence signal of the sample algae due to the decrease in transmission at DW. However, this does not significantly alter the fluorescence induction curve or the determinations of  $\sigma_{\text{PSII}}$  and  $F_v/F_m$ .

#### *SOW-FRRF*

In SOW-FRRF, biofilm attains real  $F_m$  hence  $\sigma_{\text{PSII}}$  will not remain the same as that of the sample (i.e.  $\sigma_{\text{PSII}}$  will be variable) unlike in DOW-FRRF. However, in the presence of NDF on the OW, the  $\sigma_{\text{PSII}}$  values decreased linearly with decrease in transmission compared to control (Figure 8). This is because the NDF delays PSII saturation of the sample algae due to the decrease in the intensity of excitation light and the fluorescence signals ( $F_0$  and  $F_m$ ; Figure 6b).

#### ***Correction for the FRRF data affected by the initial development of the biofilms***

Through the knowledge of biofilm characteristics (transmission and chlorophyll) and blank measurements (made before and after cleaning of biofilms from the OW), a correction can be applied by using the following derived equations and recommendations. For instance, if FRRF measurement of a sample (S) is made in presence of biofilm (B) on OW, then the resultant signal will be the summation of B and S. This relation is expressed in the following equation

$$F^{B+S} = F^B + F^S \quad \text{Equation 1}$$

Wherein  $F$  stands for fluorescence and can be  $F_0$  or  $F_m$ ;  $F^{B+S}$  is the fluorescence of the sample with biofilms and  $F^B$  is the biofilm fluorescence.  $F^B$  is calculated using equation 2 through the measurement of seawater (either filtered or natural or culture) with biofilms ( $F^{B+}$ ) and without biofilms ( $F^{B-}$ )

$$F^B = F^{B+} - F^{B-} \quad \text{Equation 2}$$

$F^S$  is the fluorescence of the sample and can be calculated by rearranging the equation (1).

$$F^S = F^{B+S} - F^B \quad \text{Equation 3}$$

Using above equation it is possible to derive the correct values for  $F_0$  and  $F_m$  and using this the correct values for  $F_v$  and  $F_v/F_m$  can be calculated. From equations (2) or (3) it is also possible to calculate the proportions of the biofilm ( $x^B$ ) and sample ( $x^S$ ) fluorescence assuming  $F^{B+S} = 1$  (this can also be expressed as  $1 = x^{B+S}$ ) through the equation 3 which are essential for  $\sigma_{PSII}$  calculation.

$$F^{B+S} = 1 = x^{B+S} = x^B + x^S \quad \text{Equation 4}$$

The correction for the  $\sigma_{PSII}$  is not straightforward as with the fluorescence. However, the expected  $\sigma_{PSII}$  for the sample was obtained by weighting the fluorescence signal as described by Suggett et al. (2004) by mixing of two microalgal cultures (see equation 5, with slight modifications in Equation 6).

$$\text{Expected } \sigma_{PSII} = \frac{x1.Fm1.\sigma_{PSII1} + x2.Fm2.\sigma_{PSII2}}{x1.Fm1 + x2.Fm2} \quad \text{Equation 5}$$

Where  $x1$  and  $x2$  are the proportions of microalgal culture 1 and 2 in the mixture respectively,  $F_{m1}$  and  $F_{m2}$  are the maximum fluorescence yields of cultures 1 and 2 prior to mixing and  $\sigma_{PSII1}$  and  $\sigma_{PSII2}$  are the initial effective absorption cross sections prior to mixing.

$$\sigma_{PSII B + S} = \frac{xB.FmB.\sigma_{PSIIB} + xS.FmS.\sigma_{PSIIS}}{xB.FmB + xS.FmS} \quad \text{Equation 6}$$

The equation 6 is rearranged for the calculation of  $\sigma_{PSII}$  of the sample ( $\sigma_{PSIIS}$ ) and biofilms ( $\sigma_{PSIIB}$ ) and  $xB$  and  $xS$  are the proportions corresponding to biofilm and samples.

$$\sigma_{PSIIS} = \frac{\{\sigma_{PSII B+S}(xB.FmB + xS.FmS)\} - (xB.FmB.\sigma_{PSIIB})}{xS.FmS} \quad \text{Equation 7}$$

$$\sigma_{PSIIB} = \frac{\{\sigma_{PSII B+S}(xB.FmB + xS.FmS)\} - (xS.FmS.\sigma_{PSIIS})}{xB.FmB} \quad \text{Equation 8}$$

Wherein,  $\sigma_{\text{PSIIB+S}}$ ,  $\sigma_{\text{PSIIS}}$  and  $\sigma_{\text{PSIIB}}$  are the effective absorption cross section of the sample with biofilm, only sample and biofilm, respectively.  $\sigma_{\text{PSIIB}}$  can be calculated through the measurement of seawater (either filtered or natural) with or without biofilms. Equations (7) and (8) should be used only when filtered seawater and natural seawater are used for correction, respectively. However, the use of equation 7 and 8 for correction should be made with caution depending on the fluorescence values. Since  $\sigma_{\text{PSII}}$  of the sample with and without biofilm remained same (or real  $F_m$  is not attained), with DOW-FRRF the correction procedure for  $\sigma_{\text{PSII}}$  proposed (Equations 5 to 8) are applicable only for SOW-FRRF.

### **Conclusions**

Simulation of biofouling on the FRRF OWs was effective in addressing the biofouling influence on its performance. The approach is simple, cost effective and involves no risk (eg: damage to OWs). Simulation experiments revealed that the biofilms with chl *a* containing organisms on the DW influenced the quality of fluorescence data ( $F_0$ ,  $F_m$  and  $F_v/F_m$  values) by interfering with the sample fluorescence signals. Biofilms with chl *a*  $>0.1\mu\text{g cm}^{-2}$  on SOW FRRF and  $>0.3\mu\text{g cm}^{-2}$  on the DW of DOW-FRRF are critical in measurements. However, if biofilm on DW is dominated by non-chlorophyll containing organisms, a reduced sample fluorescence signal is detected due to the reduction in the transmission. Here the correction (for SOW- and DOW-FRRF) procedures for  $F_v$ ,  $F_v/F_m$  and  $\sigma_{\text{PSII}}$  are also proposed. In DOW-FRRF, biofilm at EW reduced the flash intensity and influenced the data quality only if there was a significant decrease in the optical transmission. These observations suggest that biofouling on the optical instruments can significantly affect the data quality during extended deployments. Hence, implementation of antifouling measures is a prerequisite for optical instruments especially to ensure retrieval of quality data. In DOW-FRRF, antifouling source should be placed towards the DW. Considering fouling on DW, if possible, the following improvements in the instruments optical configuration are recommended: 1) collimation of excitation light to minimize illumination on DW; 2) blocking of DW from excitation light without interfering with the signal detection and 3) use of high intensity light source to compensate for reduction in flash intensity due to fouling on EW.

### **Acknowledgements**

First author, J.S.P., gratefully acknowledges the Japanese Government Scholarship (Monbukagakusho) provided by Ministry of Education, Science, Sports and Culture, Government of Japan and to the

Government of India for nominating for the scholarship. We thank the Director, CSIR-National Institute of Oceanography (CSIR-NIO) and Dr. AC Anil CSIR-NIO, Goa, India for support and encouragement. We also thank Dr. SS Sawant for his constructive suggestions. We also thank two anonymous reviewers for their important comments to improve the manuscript. This paper is a NIO contribution.....

## References

- Cooksey KE, Wigglesworth-Cooksey B. 1995. Adhesion of bacteria and diatoms to surfaces in the sea: a review. *Aquat Microb Ecol.* 9: 87–96.
- Dubinsky Z. 1992. The functional and optical absorption cross-sections of phytoplankton photosynthesis. In: Falkowskii PG, Woodhead AD, editors. Primary productivity and biogeochemical cycles in the sea. New York: Plenum Press.; p. 31-45.
- Falkowski PG, Kolber Z. 1995. Variations in chlorophyll fluorescence yields in phytoplankton in the world oceans. *Aust J Plant Physiol.* 22: 341–355.
- Fujiki T, Hosaka T, Kimoto H, Ishimaru T, Saino T. 2008. *In situ* observation of phytoplankton productivity by an underwater profiling buoy system: use of fast repetition rate fluorometry. *Mar Ecol Prog Ser.* 353: 81-88.
- Fujiki T, Matsumoto K, Watanabe S, Hosaka T, Saino T. 2011. Phytoplankton productivity in the western subarctic gyre of the North Pacific in early summer 2006. *J Oceanogr.* 67 (3): 295-303.
- Gorbunov MY, Kolber ZS, Lesser MP, Falkowski PG. 2001. Photosynthesis and photoprotection in symbiotic corals. *Limnol Oceanogr.* 46(1): 75–85
- Greene RM, Geider RJ, Falkowskii PG. 1992. Effect of iron limitation on photosynthesis on a marine diatom. *Limnol Oceanogr.* 36: 1772-1782.
- Guillard RRL, Ryther JH. 1962. Studies of marine planktonic diatoms. I. *Cyclotella nana* Hustedt, and *Detonula confervaceae* (Cleve Gran). *Can J Microbiol.* 8: 229-239.
- Kaiblinger C, Dokulil MT. 2006. Application of fast repetition rate fluorometry to phytoplankton photosynthetic parameters in freshwaters. *Photosynth Res.* 88: 19–30.
- Kerr A, Cowling MJ, Beveridge CM, Smith MJ, Parr ACS, Head RM, Davenport J, Hodgkiess T. 1998. The early stages of marine biofouling and its effect on two type of optical sensor. *Environ Int.* 24: 331–343.
- Kolber Z, Falkowskii PG. 1993. Use of active fluorescence to estimate phytoplankton photosynthesis *in situ*. *Limnol Oceanogr.* 38: 1646-1665.
- Kolber Z, Zehr J, Falkowskii PG. 1988. Effects of growth irradiance and nitrogen limitation on photosynthetic energy conversion in photosystem II. *Plant Physiol.* 88: 923-929.



- Kolber Z, Wyman KD, Falkowskii PG. 1990. Natural variability in photosynthetic energy conversion efficiency: a study in the Gulf of Maine. *Limnol Oceanogr.* 35: 72-9.
- Kolber Z, Ondrej P, Falkowskii PG. 1998. Measurements of variable chlorophyll fluorescence using fast repetition rate techniques: defining methodology and experimental protocols. *BiochimBiophysActa.* 1367:88-106
- Krause GH, Weis E. 1991. Chlorophyll fluorescence and photosynthesis: The basics. *Annu Rev Plant Physiol Plant Mol Biol.* 42:313-349.
- Lesser MP, Gorbunov MY. 2001. Diurnal and bathymetric changes in chlorophyll fluorescence yields of reef corals measured *in situ* with a fast repetition rate fluorometer. *Mar Ecol Prog Ser.* 212: 69–77.
- Ley AC, Mauzerall D. 1982. Absolute absorption cross-sections for photosystem II and the minimum quantum requirement for photosynthesis on *Chlorella vulgaris*. *BiochimBiophysActa.* 680:95-106.
- Mauzerall D, Green-Baum NL. 1989. The absolute size of a photosynthetic unit. *Biochim Biophys Acta.* 974: 119-140.
- Moore CM, Lucas MI, Sanders R. Davidson R. 2005. Basin-scale variability of phytoplankton bio-optical characteristics in relation to bloom state and community structure in the Northeast Atlantic. *Deep Sea Res I.* 52: 401–419.
- Moore CM, Suggest D, Holligan PM, Sharples J, Abraham ER, Lucas MI, Rippeth TP, Fisher NR, Simpson JH, Hydes DJ. 2003. Physical control on phytoplankton physiology and production at a shelf sea front: a fast repetition-rate fluorometer based field study. *Mar Ecol Prog Ser.* 259: 29–45.
- Miller RJ, Dessureault JG, Beanlands BD, SharpGJ. 1996. Benthic temperature, light and water speed (TLS) recorder. *J Expt Mar BiolEcol* 205:83-89.
- MinoY, Matsumura S, Lirdwitayaprasit T, Fujiki T, Tetsuoyanagi, SainoT. 2013. Variations in phytoplankton photo-physiology and productivity in a dynamic eutrophic ecosystem: a fast repetition rate fluorometer-based study. *J Plankt Res.* 36 (2): 398-411.
- Patil JS, Kimoto H, Kimoto T, Saino T. 2007. Ultraviolet radiation (UV-C): a potential tool for the control of biofouling on marine optical instruments. *Biofouling.* 23:215–230.
- Patil JS, Jagadeesahn V. 2011. Effect of chlorination on the development of marine biofilms dominated by diatoms. *Biofouling.* 27 (3):241–254.
- Schoellhamer DH. 1993. Biological interference of optical back scatterance sensors in Tampa Bay, Florida. *Mar Geol.* 110: 303-313.
- Suggest DJ, MacIntyre HL, Geider RJ. 2004. Evaluation of biophysical and optical determinations of light absorption by photosystem II in phytoplankton. *Limnol. Oceanogr.: Methods.* 2: 316–332
- Suzuki R, Ishimaru T. 1990. An improved method for the determination of phytoplankton chlorophyll using N, N-dimethylformamide. *J Oceanogr Soc Japan.* 46:190-194.

## Figure legends

Fig. 1. Photographs of different versions of Fast repetition rate fluorometer (FRRF) along with exploded view of optical windows (a and b) and fluorescence transients (c) used in the experiments. (a) Double optical windows (DOW) type FRRF - FAST<sup>tracka</sup> (b) Single optical window (SOW) type FRRF – FastOcean fluorometer and c: FRR fluorescence transients observed during a single turnover flash followed by a relaxation protocol. The ST protocol consisted of 100 flashlets with an interval of 1  $\mu$ s. The relaxation protocol consisted of 40 flashlets at 20  $\mu$ s intervals.  $F_0$ ,  $F_m$  and  $F_v$  ( $=F_m - F_0$ ) are the initial, maximal and variable fluorescence respectively whereas  $\sigma$ PSII is the functional absorption cross section of photosystem II.

Fig. 2. Flow chart describing in detail the mode of (a) SOW-FRRF and (b) DOW-FRRF operations to evaluate the effect of natural biofilms containing chlorophyll on the measurements. Note: The type of natural biofilms (freshwater NB for DOW-FRRF and marine NB for SOW-FRRF) used will not be an issue on the outcome of the results as performance of FRRF depends only on the status of chlorophyll in the biofilm.

Fig. 3. Details of biofilm transmission spectra (a. fouled cover glass and b polystyrene petri dish) and chl *a* (c) used for evaluating FRRF performance. The y-axis: measured chl *a* = chl *a* measured with Turner fluorometer and estimated chl *a* = chl *a* estimated from the relationship between measured chl *a* vs biofilm transmission at 680 nm.

Fig. 4. DOW-FRRF measurements of microalga *Isochrysis galbana* (at chl concentration of 1-2 mg m<sup>-3</sup>) in the presence of different levels of natural biofilm transmission and chlorophyll on both excitation and detection windows. Note: (1) Biofilm chlorophyll is calculated using the linear relationship (biofilm chlorophyll=2.4471\* $F_0^B$ -0.3176, r=0.9993, n=5) obtained from the data presented in Table 1b, (2) the chlorophyll concentrations of the sample used for the measurements were ranged between 0.97 to 1.55 mg m<sup>-3</sup> and is calculated using the linear relationship equation [(Calculated Chl = (0.326 \*  $F_0$ )-0.127); r = 0.9975] obtained between the FRRF measurements ( $F_0$ ; a proxy for chlorophyll) and measured chlorophyll of *Isochrysis galbana* cultures and (3)  $F_0$ ,  $F_m$  and  $F_v$  are recorded in arbitrary units whereas  $F_v/F_m$  is dimensionless.

Fig. 5. DOW-FRRF measurements of microalga *Isochrysis galbana* in the presence of different levels of natural biofilm transmission and chlorophyll only on excitation window (EW) and detection window (DW). Note:  $F_0$ ,  $F_m$  and  $F_v$  are recorded in arbitrary units whereas  $F_v/F_m$  is dimensionless.

Fig. 6. SOW-FRRF measurement of microalga *Isochrysis galbana* in the presence of (a) natural biofilms (NB) of different transmission and chlorophyll levels and (b) neutral density filters (NDF) of different transmission levels on single optical window. Note: (1) Biofilm chlorophyll is calculated using the linear relationship (Biofilm chlorophyll =  $0.039 * F_0^B + 0.0993$ ,  $r=0.9771$ ,  $n=7$ ) obtained from the data presented in Table 1a; (2) the microalga chlorophyll concentrations (determined by SOW-FRRF software) used for measurements were  $10.9$  and  $2 \text{ mg m}^{-3}$  with NB and NDF measurements, respectively and (3)  $F_0$ ,  $F_m$  and  $F_v$  are recorded in arbitrary units whereas  $F_v/F_m$  is dimensionless.

Fig. 7. Performance of DOW-FRRF in the presence of neutral density filters (NDF) of different transmission levels on both excitation and detection windows. Note:  $F_0$ ,  $F_m$  and  $F_v$  are recorded in arbitrary units whereas  $F_v/F_m$  is dimensionless.

Fig. 8. Performance of DOW-FRRF in the presence of neutral density filters (NDF) of different transmission levels only on excitation window (EW) and detection window (DW). Note:  $F_0$ ,  $F_m$  and  $F_v$  are recorded in arbitrary units whereas  $F_v/F_m$  is dimensionless.

Table 1. Effect of natural biofilms (placed on optical windows of DOW-FRRF and SOW-FRRF) on FRRF measurements ( $F_0$  and  $F_m$ ) made in bench top mode using filtered seawater as the sample. Bold values indicate the values significantly different from the control values (T-Test;  $p < 0.01$ ). EW – Excitation window; DW – Detection window; BW – Both windows; Note: Units of  $F_0$  and  $F_m$  are recorded in arbitrary units.

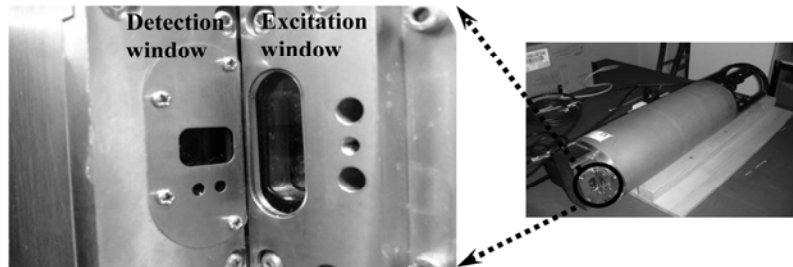
a. SOW-FRRF

Transmission %	Biofilm chl <i>a</i> $\mu\text{g cm}^{-2}$	$F_0$	$F_m$
100 (Control)	blank	0.630	0.650
96.27	0.15	<b>3.290</b>	<b>4.930</b>
93.87	0.24	<b>2.700</b>	<b>4.100</b>
92.51	0.37	<b>4.600</b>	<b>8.300</b>
91.96	0.42	<b>8.390</b>	<b>15.820</b>
77.93	1.99	<b>54.500</b>	<b>73.800</b>
75.42	2.03	<b>40.500</b>	<b>101.700</b>

b. DOW-FRRF

Transmission %	Biofilm chl <i>a</i> $\mu\text{g cm}^{-2}$	$F_0$			$F_m$		
		EW	DW	BW	EW	DW	BW
100 (Control)	blank	0.183	0.183	0.183	0.213	0.213	0.213
99.02	0.28	0.159	0.225	0.210	0.169	0.235	0.220
98.53	0.59	0.187	<b>0.469</b>	<b>0.409</b>	0.200	<b>0.478</b>	<b>0.418</b>
98.49	1.01	0.190	<b>0.686</b>	<b>0.482</b>	0.202	<b>0.694</b>	<b>0.491</b>
94.70	7.73	<b>0.572</b>	<b>3.063</b>	<b>3.292</b>	<b>0.649</b>	<b>3.067</b>	<b>3.297</b>

(a) Fast tracka: Double optical window (DOW) type FRRF



(b) FastOcean: Single optical window (SOW) type FRRF



(c) Fluorescence transient

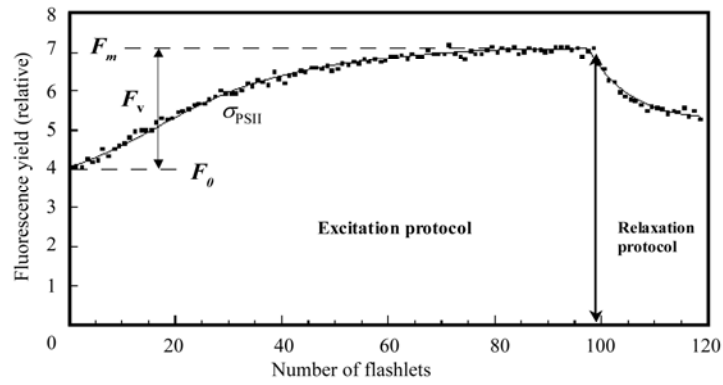


Figure 1.

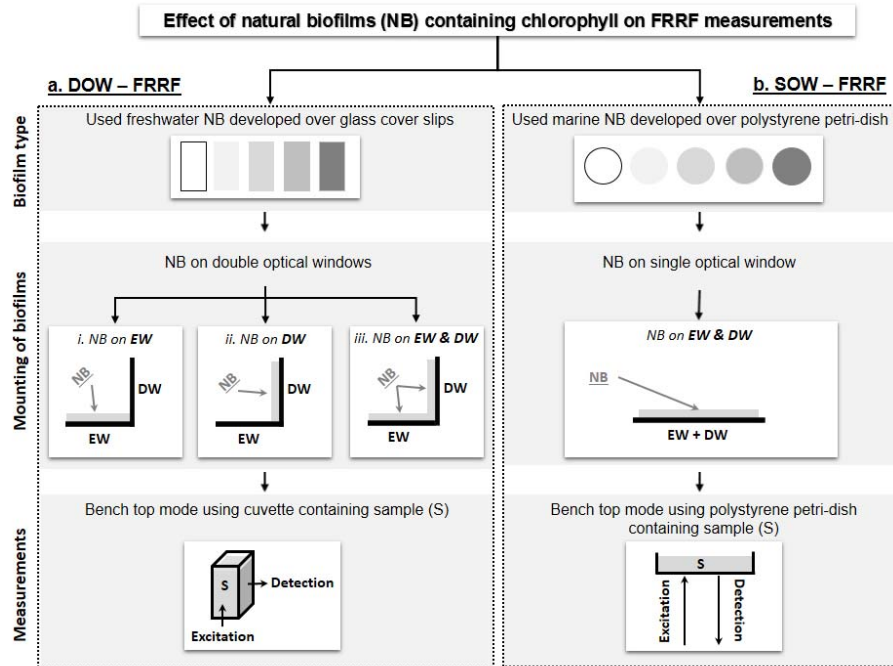


Figure 2.

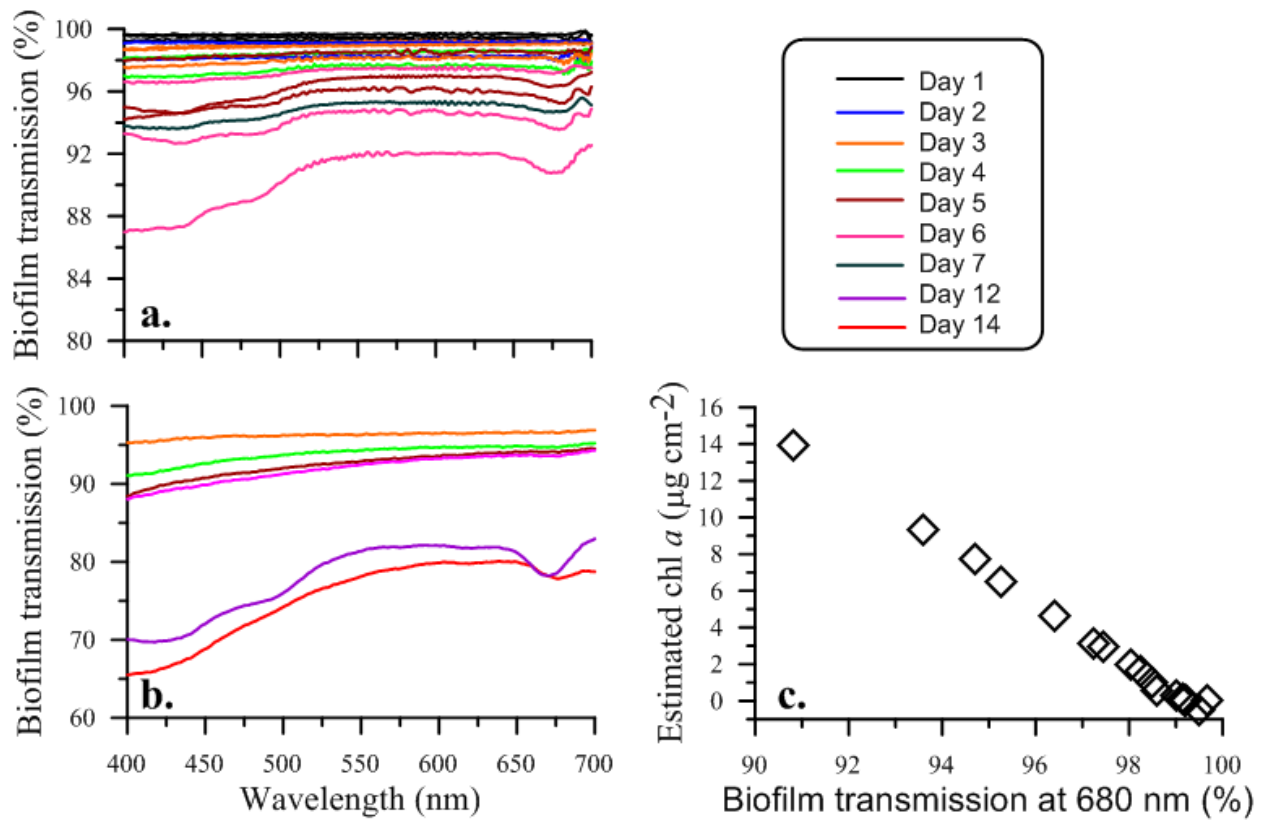


Figure 3

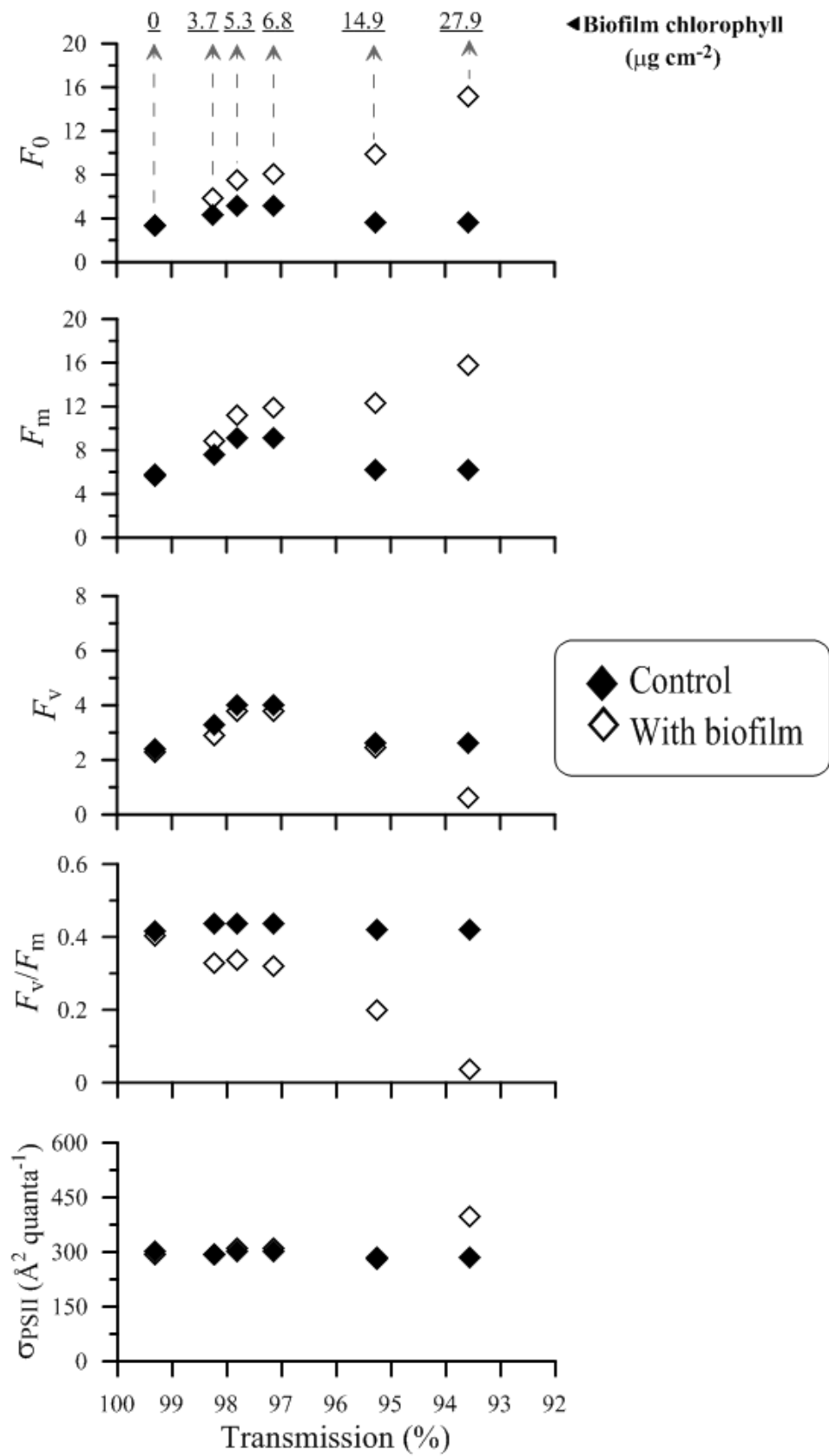


Figure 4



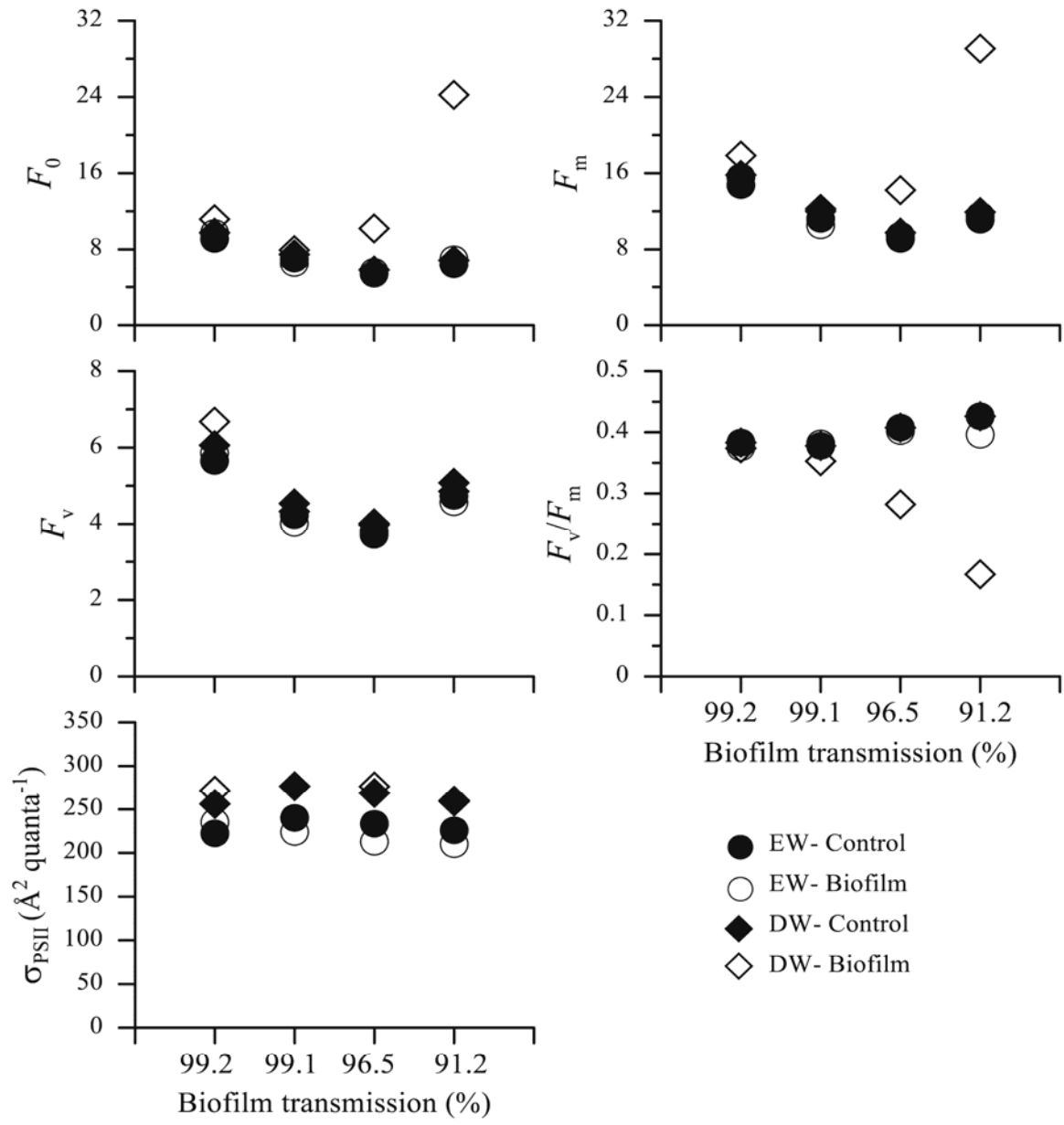


Figure 4.

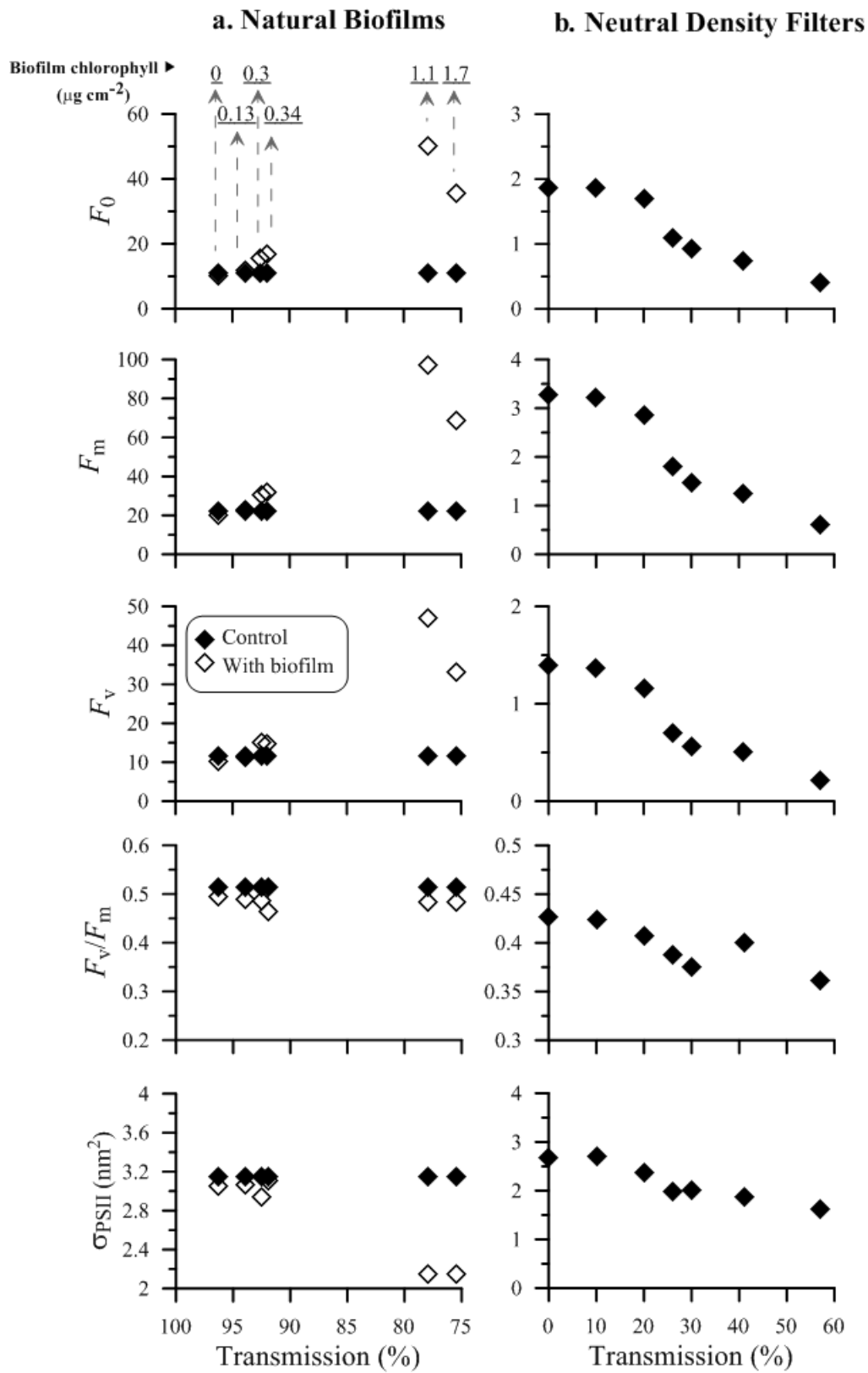


Figure 6

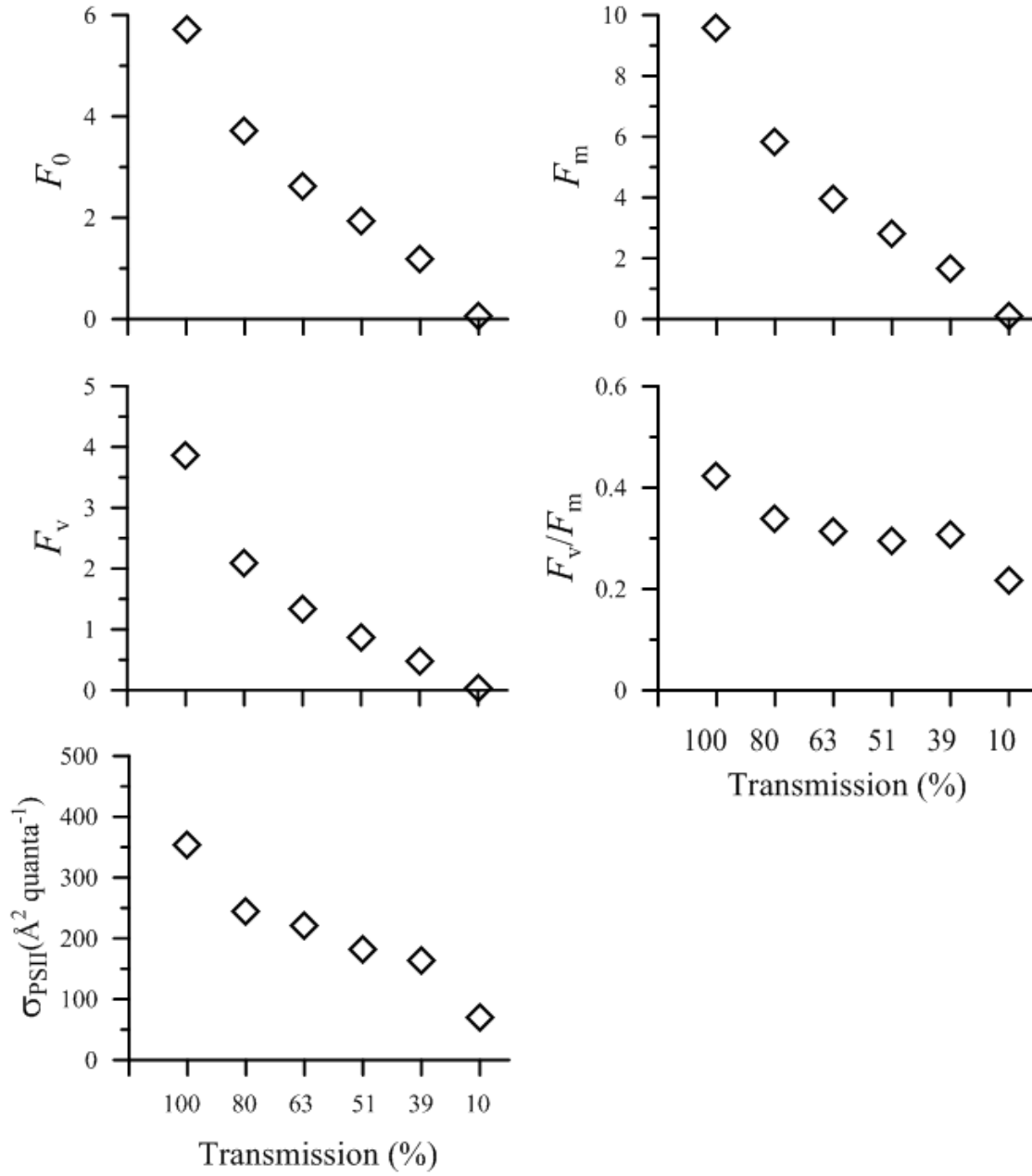


Figure 7

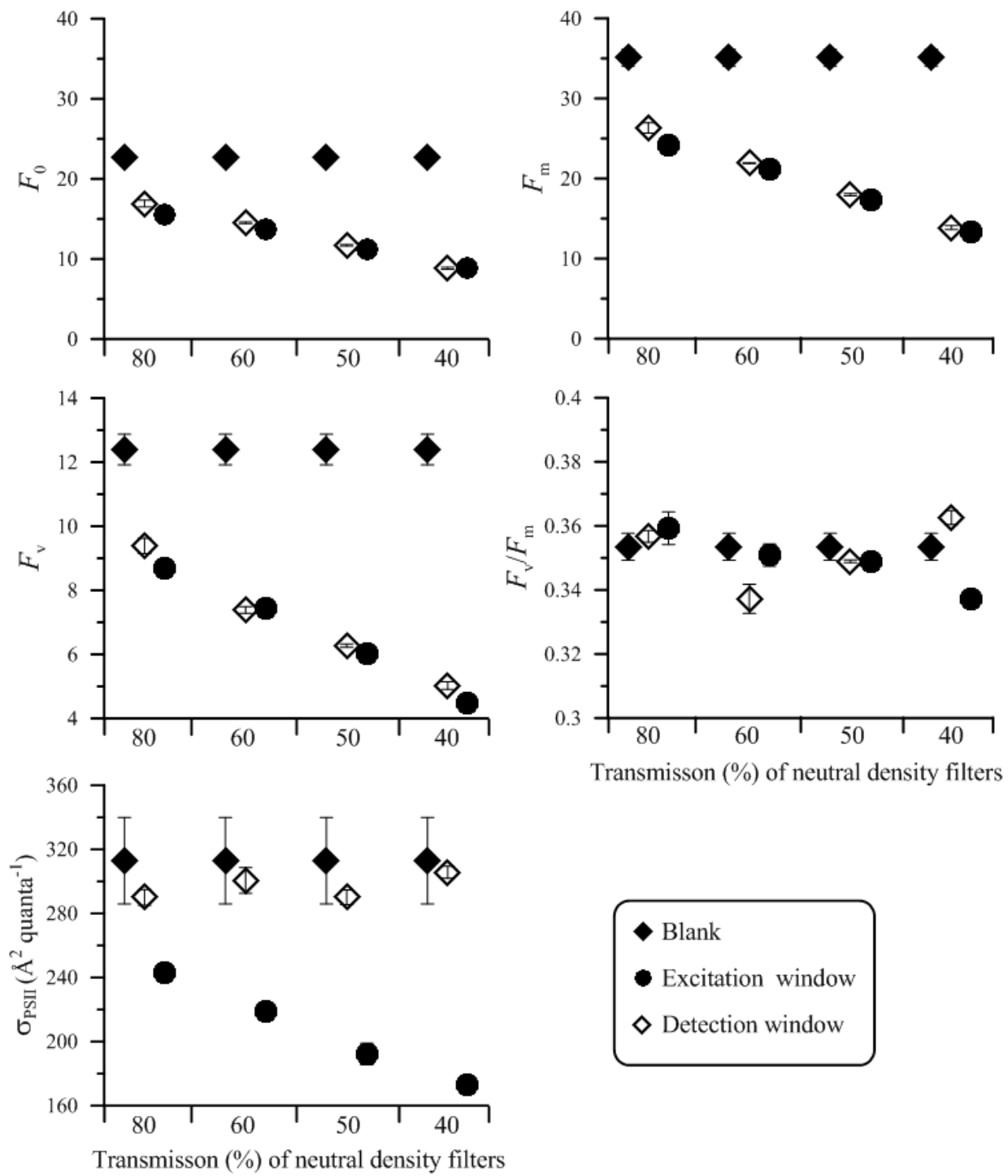


Figure 8.